Tuning the Effective Work Function of Gold and Silver Using ω-Functionalized Alkanethiols: Varying Surface Composition through Dilution and Choice of Terminal Groups

Dana M. Alloway,[†] Amy L. Graham,[†] Xi Yang,[†] Anoma Mudalige,[†] Ramon Colorado, Jr.,[‡] Vicki H. Wysocki,[†] Jeanne E. Pemberton,[†] T. Randall Lee,[‡] Ronald J. Wysocki,[†] and Neal R. Armstrong*[,†]

Department of Chemistry, University of Arizona, Tucson Arizona 85721, and Department of Chemistry, University of Houston, Houston, Texas 77204-5003

Received: October 02, 2009; Revised Manuscript Received: October 08, 2009

Thiol-based self-assembled monolayers (SAMs) have been used to tune the effective work function of gold over a range of ca. 1.8 eV via two strategies: (i) the use of ω-functionalized alkanethiols where the tail groups have widely varying electronegativity or (ii) by the creation of two-component SAMs from selected mixtures of methyl-terminated alkanethiols (**C16**) and alkanethiols fluorinated at the two terminal carbon atoms (**C16F2**). UV-photoelectron spectroscopy (UPS) was used to monitor changes in effective work function, using shifts in the low kinetic energy edge of these photoemission spectra to quantify the shift in local vacuum level resulting from the interface dipole effect created by the surface modifier. Tail groups on alkanethiol chains varied from $-CH_3$, to −phenyl, −Cl, −Br, and $-CF_3$ or $-CF_2CF_3$, which provided a shift in local vacuum level that varied linearly with the calculated molecular dipole moment of the individual modifiers, as observed previously for a more limited range of alkanethiols (*J. Phys. Chem. B* **2003**, *107*, 11690). The studies presented here confirm that the intrinsic dipole in the gold−thiolate bond is small (less than 100 meV), whereas the silver−thiolate bond appears to have a strongly polar character, in the direction Ag^+-S^- (ca. 900 meV). The use of a simple point dipole model to rationalize these apparent shifts in vacuum level was further explored using SAMs derived from various mixtures of **C16** and **C16F2**. The low kinetic energy edge in the UV-photoemission spectra and the effective work function are observed to increase monotonically in energy with increasing **C16F2** coverage, confirming that little surface segregation occurs in these self-assembled monolayers over a wide concentration range.

Introduction

Tuning of the effective work function of metal and semiconductor surfaces using molecular adsorbates is an area that has seen increased emphasis, owing to the importance of metal/organic and semiconductor/organic interfaces in emerging molecular electronic technologies.[1−43] Over the past two decades, several model studies have been conducted in which simple adsorbates, such as alkanethiols on coinage metals, and various carboxylates, phosphonates, and silanes on metal oxide surfaces, are added to these surfaces at monolayer or submonolayer coverages.[1,3,4,6,8,9,14,19,20,22−34,40,43,44] The subsequent shifts in effective work functions, as measured by Kelvin probe or UV-photoemission spectroscopy (UPS), have shown simple correlations with the molecular dipole moment of the adsorbate, and the formation of an "interface dipole".[10−16,45,46] The impact of these adsorbates on the current/voltage properties of simple diodes and transistors is significant. Single monolayers of certain molecules can alter the onset voltages, leakage currents, rectification ratios, and quality factors of simple diodes and greatly alter the subthreshold slopes, saturation currents, and drive frequencies of organic field-effect transistors.[4,10−16,47−52]

The influence that these interface dipoles exert on ion neutralization, using the chemically modified surface for surface-induced dissociation mass spectrometry (SID), is also of interest.[53] The appropriate choice of surface modifier can alter the neutralization probability of an incoming positive ion by at least an order of magnitude and might also alter the course of SID reactions that involve more than fragmentation (e.g., deposition of diatomic fragments and atom exchange).

Previous work from this group has focused on the use of UPS to monitor the change in work function of a series of gold surfaces modified with normal alkanethiols of different lengths, and 16-carbon alkanethiols fluorinated at the terminal methyl position (**C16F1**), the terminal ethyl position (**C16F2**), the last 4 carbon atoms (**C16F4**), and the last 10 carbon atoms (**C16F10**).[6] Assuming electronic equilibrium between the SAM modifier and the underlying gold surface, the shift in the low kinetic energy edge of the photoemission spectrum was used as an indicator of changes to effective work function, where the width of the photoemission spectrum, from the Fermi edge photoemission energy for gold to the low KE edge, subtracted from the source energy (He(I) = 21.2 eV), provides the effective work function.[15,17] We have recently extrapolated these studies to the modification of indium−tin oxide (ITO) surfaces with dipolar phosphonic acids (PA), where similar correlations are observed between molecular dipole moment and shift in effective surface work function for a group of fluoroalkyl PAs and more recently fluorinated aromatic PAs.[8,9]

On Au surfaces, we initially showed that there was a simple correlation between the molecular dipole moment of the

* To whom correspondence should be addressed. Phone: 520-621-8242. Fax: 520-621-8407. E-mail: nra@u.arizona.edu.
[†] University of Arizona.
[‡] University of Houston.

10.1021/jp909494r CCC: $40.75
Published on Web 10/29/2009

alkanethiol modifier and the shift in local vacuum level as revealed by shifts in the low kinetic energy (KE) edge of the UV-photoemission spectrum. Gaps in this correlation have now been filled in with new modifiers that are presented here. The improved linear correlation provides more confidence that the intrinsic shift in vacuum level for any alkanethiol modifier on Au surfaces is ca. 0.4 eV, the same as has been observed for a noninteracting species such as adsorbed xenon gas.[54,55] This observation further implies that the intrinsic dipole moment in the gold−thiolate bond is small (±0.05 V), a conclusion that has also been recently reached by De Renzi and co-workers, as well as other groups, using smaller alkanethiols adsorbed from the gas phase.[5]

SAMs formed by the adsorption of alkanethiols on silver have also been extensively studied, and their properties have been compared to those of SAMs formed from the corresponding molecules on gold.[44,56] In the present work, we repeat the UPS study of vacuum level shift vs molecular dipole moment for a variety of substituted alkanethiols on silver. The results confirm the strong differences between gold−thiolate and silver−thiolate bonding.[24,33] Interestingly, if we compute the change in effective surface work function per unit change in molecular dipole moment, ($\Delta\Phi/\Delta D$), for alkanethiols on both Au, and Ag, and various alkyl- and aryl-phosphonic acids on ITO surfaces, we obtain nearly the same slope for all three substrate materials.[9]

To examine in greater detail whether simple molecular dipole models can provide some predictability in tuning of the effective work function of coinage metals, we also modified Au surfaces with mixtures of hydrocarbon and semifluorinated alkanethiols, varying the molecular percentage of each modifier over a wide range of concentrations. It appears from these studies that (i) no appreciable segregation of these modifiers occurs,[57] (ii) the shift in the low KE edge of the photoemission spectrum and the change in effective work function are predicted by a simple linear addition of the molecular dipole moments for each modifier (i.e., the superposition principle applies), and (iii) the effective work function of Au can be tuned over a range of ca. 1.8 eV.

Experimental Section

Thiol Adsorbates. The thiols used in the mixed monolayer experiments were hexadecanethiol, $CH_3(CH_2)_{15}SH$ (**C16**), and 15,15,16,16,16-pentafluorohexadecanethiol, $CF_3CF_2(CH_2)_{14}SH$ (**C16F2**). The **C16** and other nonfluorinated alkanethiols were purchased from Aldrich (99%) and used without further purification. **C16F2** was synthesized and purified according to the reported procedure.[53,57−59] The phenyl-terminated alkanethiols, 12-phenyldodecanethiol (**C12ph**), brominated and chlorinated alkanethiols, 12-bromododecanethiol (**C12Br**) and 12-chlorododecanethiol (**C12Cl**), were synthesized in the Chemical Synthesis Facility at the University of Arizona and purified according to the reported literature.[57]

Thiol solutions were first prepared separately for each compound in absolute ethanol at a concentration of 10^{-3} M. Solutions with various molar ratios were prepared by mixing pure 1 mM thiol solutions in appropriate volume ratios. Solutions for modification of gold surfaces were prepared in ratios (**C16/C16F2**) of 0:100, 5:95, 10:90, 20:80, 30:70, 40:60, 50:50, 60:40, 70:30, 80:20, 90:10, 95:5, and 100:0.

Sample Preparation. Polycrystalline gold foils (99.95% purity, Alfa Aesar) were polished to a mirror finish, the last polishing steps used 1.0 and 0.3 μm alumina (Buehler). To remove embedded alumina, these gold foils underwent successive piranha cleaning cycles in which they were soaked in solutions of sulfuric acid (concentrated)—hydrogen peroxide (30%) mixture (4:1) for 15 min and rinsed with water and ethanol and repeated until aluminum and oxygen were no longer observed in the X-ray photoelectron spectrum. Foils were cleaned between uses following the same procedure, adding a UV-cleaning step (Boekel UV cleaner, model 135500, Boekel industries, Inc.) for 15 min. Samples were then rinsed in ethanol before being submerged in the alkanethiol solutions for 24−72 h. Mixed monolayer surfaces were all prepared with 24 h incubation times. After incubation, the surfaces were rinsed and sonicated in ethanol six times (1 min per cycle in fresh solvent), and then these samples remained submerged in ethanol before being loaded into the vacuum chamber for analysis by XPS and UPS.

Silver surfaces were formed from a solid silver disk having a diameter of 1 cm and were mechanically polished until smooth. The surfaces were prepared for alkanethiol modification as described previously,[60−62] by mechanical polishing (1.0 and 0.3 μm alumina) followed by a chemical polish (solvent soak and combination of acid treatment, chromia/HCl, base treatment with water rinses in between). Substrates were then hydrogen-flame annealed and soaked in DI water as described previously. Silver surfaces were checked via ellipsometry for a lack of significant oxidation before soaking in alkanethiol solutions and then re-examined by ellipsometry for complete removal of nonbonded molecules, after SAM formation. Surfaces were soaked for 24 h in 1−2 mM alkanethiol solutions (in ethanol) for SAM formation.

Photoelectron Spectroscopy Measurements (X-ray and UV). Photoelectron spectroscopy was performed in a Kratos Axis Ultra UPS/XPS spectrometer. XPS data were collected using the monochromatic Al Kα source at a pass energy of 20 eV for high-resolution spectra and 80 eV for survey scans. UPS spectra were acquired with a 21.2 eV He(I) source (Specs UVS 20-A UV discharge source) at a pass energy of 5 eV. In the UPS experiments, a −5 or −9 V bias was applied to the sample to increase the kinetic energy of all photoelectrons, improving the instrument response and resolution of the low KE electrons.[6,63−65] At the beginning of each day of data collection, XPS and UPS were collected for an atomically clean, polycrystalline gold foil to ensure instrument consistency and to have a standard with which to compare modified Au and Ag surfaces.

Results and Discussion

UPS Data for Gold Surfaces Modified with Various Thiols. Figure 1a shows a schematic view of the thiol adsorbates used in these photoemission experiments. These molecules were chosen to vary the magnitude and sign of the molecular dipole moment over a wide range in a systematic fashion and complement those chosen in our earlier studies.[6] Modifiers included (a) 16-carbon thiols with fluorination at the terminal 2, 4, and 10 carbons, designated **C16F2**, **C16F4**, and **C16F10**, respectively, along with the normal C16 alkanethiol (**C16**); the phenyl-terminated C12-alkanethiol (denoted **C12ph**); and (c) the singly brominated and chlorinated C12-alkanethiols (denoted **C12Br** and **C12Cl**). It is conceivable, given earlier work of a similar nature, that the range of interface dipoles could have been even larger if an amine group had been added to this series, as was shown by Campbell and co-workers.[45,46]

Figure 1b and c provides a sample of UPS data obtained for clean Au and Au surface modified with a range of alkanethiols, including examples of UPS data obtained for mixed SAMs derived from varying **C16/C16F2** ratios (see below). Similar data for modified Ag surfaces are shown in Figure 2. Molecular

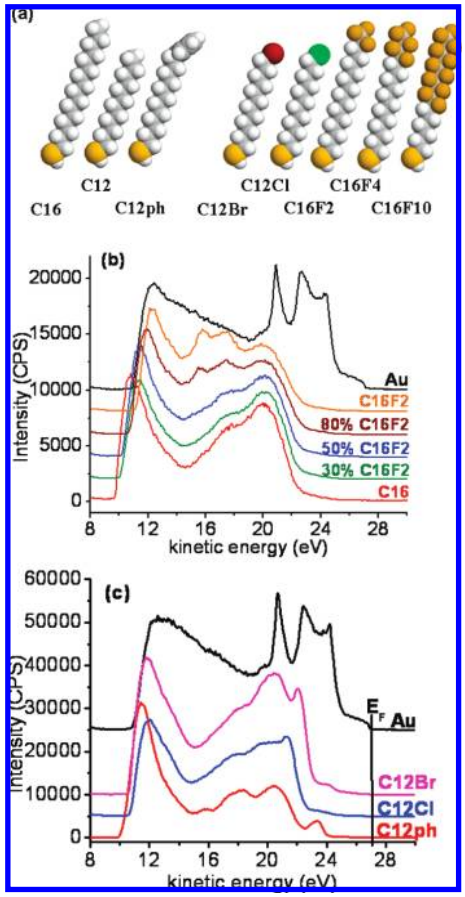

Figure 1. (a) Schematic views of the alkanethiols used in this study with different end groups, including methyl, phenyl bromo, chloro, and semifluorinated functional groups; (b, c) UV-photoelectron spectra for (b) clean Au and Au modified with 100% **C16**, 100% **C16F2**, and variable percentages of **C16F2** diluted into the C16 host layer (see additional data for mixed monolayers in Figure 5) and (c) clean Au and Au modified with −Br, −Cl, and −phenyl-terminated C12 alkanethiols.

dipole moment data not discussed in our previous publication, for both Au and Ag surfaces, are summarized in Tables 1 and 2. For all of these modified surfaces the photoemission signal from the Fermi edge emission from the underlying gold or silver substrates was observable (with long integration times if needed), with an intensity appropriate for attenuation of its signal due to escape of photoelectrons through a pinhole free modifying layer.[6] The Au or Ag Fermi edge emission decreased exponentially with increasing length of the alkanethiol modifier, consistent with formation of densely packed modifying layers. We verified that the KE of photoemission from the Fermi level was unchanged as result of addition of the surface modifier, thus ensuring that electronic equilibrium was maintained between the modified metal surface and the spectrometer.[15,17] The effective work function of clean or modified Au or Ag surfaces is then determined from the difference in the width of the photoemission spectrum and excitation source energies (21.2 eV), and changes in effective work function were monitored from the shifts in the low KE edge of the photoemission spectrum.[15,17,63−65]

Correlation of Changes in Effective Work Function with Molecular Dipole Moment. Figure 3 shows the shift in local vacuum level observed for Au and Ag surfaces, with various alkanethiol modifiers, as a function of the calculated molecular dipole moment, projected along the normal axis (see also Table 1). The assumed orientations for these modifiers are shown in

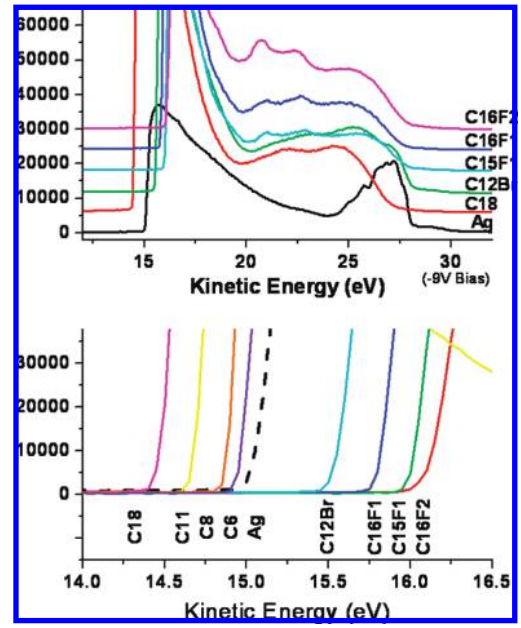

Figure 2. (upper) UV-photoelectron spectra for clean Ag and Ag surfaces modified with 100% **C18, C12Br**, **C16F1**, **C15F1**, and **C16F2**; (lower) expanded view of the low KE secondary electron edge (SEE) region of these same spectra, including **C6**, **C8**, and **C11**, to accentuate the shifts in local vacuum level brought about by surface modification.

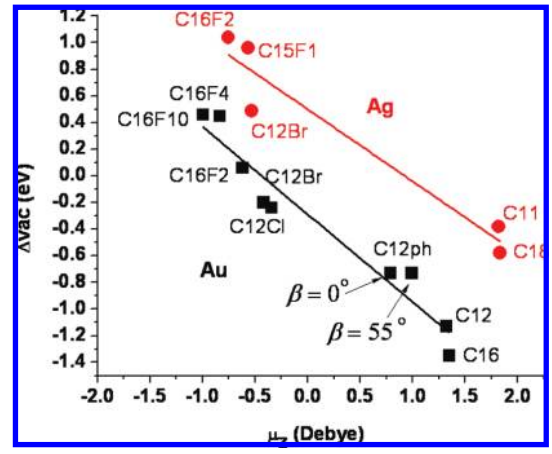

Figure 3. Observed shift in vacuum level (low KE edge of the UV-photoelectron spectra) versus the calculated molecular dipole moment of the modifier, projected along the surface normal. Square symbols (black) are alkanethiols on gold (the boxed entries are new thiols added to those previously examined by us),[12] and triangles (red) are alkanethiols on silver. The dashed lines provide an estimate of the vacuum level shift expected for an adsorbate with no molecular dipole moment (e.g., Xe adsorbed on either Au or Ag).[56,57,81,81]

Figure 4. In our previous studies, the gas-phase dipole moment of the individual molecules were calculated using Gaussian 98.[6,66] In the data shown here we updated these initial calculations and added calculations for the new SAMs, using HF geometry optimization with basis set 6-31G(d) and dipoles calculated with UHF 6-31+G(2d,p) with GAMESS (Version 24 MAR 2007).[67]

The geometry optimization was first performed on the individual molecule, the dipole calculation was completed by freezing the geometry, removing the thiol hydrogen, calculating the neutral radical dipole moment. The neutral radical was assumed to calculate the relevant dipole moment, since the thiol

TABLE 1: UPS and Calculated Dipoles for Alkanethiol Monolayers on Gold

	molecular formula	shift in effective vacuum level (eV) ± 0.1 eV	effective work function (eV) ± 0.1 eV	calculated molecular dipole moment (D)	calculated dipole projected along surface normal[a] (D)	dipole along molecule (D)	angle molecule vs dipole (°)
C12ph	$HS(CH_2)_{11}C_6H_5$	−0.8	4.1	1.77	0.99/0.79	1.55	29
C12Cl	$HS(CH_2)_{12}Cl$	−0.24	4.7	−0.51	−0.34	−0.48	18
C12Br	$HS(CH_2)_{12}Br$	−0.2	4.8	−0.60	−0.42	−0.58	16
C12	$HS(CH_2)_{12}CH_3$	−1.13	3.9	2.28	1.32	2.03	27

[a] Normal dipole moments (D) reported for 55° β twist/0° β twist for phenyl terminated alkanethiols.

TABLE 2: UPS and Calculated Dipoles for Various Alkanethiol Monolayers on Silver

	molecular formula	low KE cutoff ± 0.1 eV	ionization potential ± 0.2 eV	work-function ± 0.1 eV	Fermi edge ± 0.05 eV	vacuum level shift ± 0.1 eV	total dipole (D)	dipole normal to surface (D)	dipole along molecule (D)	angle molecule vs dipole (°)
C15F1	$HS(CH_2)_{14}CF_3$	16.01	9.31	5.18	32.03	0.96	−0.64	−0.57	−0.61	17
C16F1	$HS(CH_2)_{15}CF_3$	15.81	9.31	4.98	32.03	0.76	−2.26	−1.02	−0.72	−71
C16F2	$HS(CH_2)_{14}CF_2CF_3$	16.10	9.34	5.25	32.05	1.04	−0.80	−0.75	−0.80	7
C12Br	$HS(CH_2)_{12}Br$	15.55	8.60	4.70	32.05	0.49	−0.60	−0.53	−0.58	16
C18	$HS(CH_2)_{17}CH_3$	14.47	8.50	3.68	32.00	−0.58	2.29	1.83	2.05	26
C11	$HS(CH_2)_{10}CH_3$	14.67	8.30	3.84	32.03	−0.38	2.24	1.82	2.03	25
C8	$HS(CH_2)_7CH_3$	14.83	8.43	4.03	32.00	−0.22	2.26	1.79	2.01	27
C6	$HS(CH_2)_5CH_3$	14.95	8.24	4.16	32.00	−0.10	2.23	1.75	1.97	28

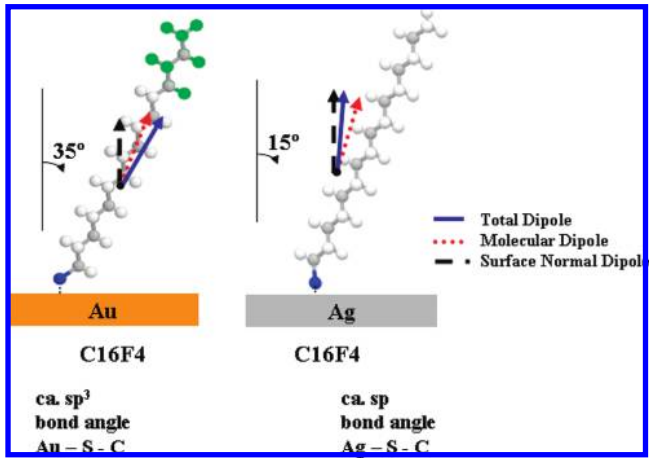

Figure 4. Schematic views of C16 alkanethiols on Au and Ag, showing the difference in assumed tilt angles. Alkanethiolates on Au result in a tilt angle of ~35° from normal, whereas on Ag the tilt angle is closer to ~15°, due to a difference in binding geometry of the metal−thiolate bond.[3]

hydrogen is known to dissociate upon alkanethiol adsorption. The dipole moments for each of the surface modifiers are listed in Table 1. The dipole moments of the alkanethiols normal to the Au surface were calculated assuming a 35° tilt angle, 55° β-twist, and sp^3 bonding geometry between surface sulfur and the first carbon atom in the chain.[6,66] For phenyl-terminated modifiers the β-twist has been found to be smaller and possibly different for odd and even chain molecules from PM-IRRAS surface vibrational spectroscopies.[57] For the C12-phenyl modifier we therefore show results for a 35° tilt angle and for an assumed 55° β-twist and for a 0° β-twist. These calculated normal dipole moments differ by ca. 0.2 D and the actual value will likely lie between the two calculated values.

On silver the geometry assumed was a 15° tilt angle, 55° β-twist, and sp bonding geometry between surface sulfur and the first carbon in the chain (Figure 4).[24,32,33,68,69] This range of possible contributions to molecular dipole moment and vacuum level shift are indicated in Figure 3. The reflection−absorption IR spectroscopic characterization of these thiols on Ag surfaces, which has not been published before, is given in Figure S4 in the Supporting Information.

Nearly 2 eV shifts in local vacuum level were observed as the electronegativity of the terminal functional groups were changed, for both Au and Ag surfaces. We note that at a molecular dipole moment of zero, these plots suggest a vacuum level shift of ca. −0.4 eV for Au surfaces, and ca. +0.5 eV for Ag surfaces (dashed lines in Figure 3).

Well-ordered dipolar monolayers have been modeled as dielectric films with multiple components, each of which contributes independently to the surface potential and the shift in local vacuum level, $\Delta\Phi_{vac}$), using variations of eq 1:[4−6,15,18,24,28,32−34,46]

$$\Delta\Phi_{vac}(\text{eV}) = eD_{\perp,\text{total}} = -Ne[D_{\perp,\text{SAM}}/\varepsilon_0\cdot\varepsilon_{\text{SAM}} + D_{\text{M-S}}/\varepsilon_0\cdot\varepsilon_{\text{M-S}}] \quad (1)$$

where N is the areal density of the modifiers (typically ca. (3−5) × 10^{14} cm^{-2}), $D_{\perp,\text{SAM}}$ is the dipole moment of the self-assembled monolayer projected along the normal axis, $D_{\text{M-S}}$ is the dipole moment of the metal−thiolate bond, ε_0 is the permittivity of vacuum, and ε_{SAM} and $\varepsilon_{\text{M-S}}$ are the dielectric constants of the self-assembled monolayer and the metal−thiolate bond, respectively. Recent studies have taken a complementary approach to the description of $\Delta\Phi_{vac}$ and have gathered ($D_{\text{M-S}}/\varepsilon_0\cdot\varepsilon_{\text{M-S}}$) into a "bond-dipole" (BD) term.[1,2,29] eq 1 may predict larger shifts in vacuum level than actually observed if the dipolar field in the modifying layer is lowered due to polarization effects within the tightly packed monolayer, an effect which appears to be more likely if the self-assembled monolayer is comprised of aromatic groups, versus alkane chains.[1,2,70−72] Similar approaches have been used to describe the shifts in local vacuum levels at chemical modified conducting oxide surfaces, using phenolic modifiers, phosphonic acids, and carboxylic acids.[8,9,27,28,73−76] As discussed below we also note that a change in surface potential is expected upon adsorption of *any* molecule to a clean metal surface (or the surfaces of other conductors, see below).[6,15,17,54,77,78]

The dipole moments calculated along the normal axis ($D_{\perp,\text{SAM}}$) are compared to the apparent vacuum level shift ($\Delta\Phi_{vac}$) calculated from the shifts in the low KE ionization edge for clean Au versus those observed for each alkanethiol modifier (Figure 3, square symbols). The plot includes data points from our previous paper on this subject,[6,66] along with the halogen-terminated and phenyl-terminated modifiers, which fill in

previously missing values of molecular dipole moment, and are boxed in blue. The new data points confirm the linear relationship established previously. These data also suggest that $\Delta\Phi_{vac} = -0.4$ eV for adsorption of a molecule or atom on clean Au with a zero dipole normal to the surface ($D_{\perp,SAM,Au} = 0$). The change in surface potential observed for physisorbed, nonpolar Xe atoms on gold surfaces has been estimated from photoemission studies to be ca. -0.45 to -0.52 eV for clean Au $\langle 100 \rangle$ and polycrystalline gold, respectively.[54,55,79−81]

The vacuum level shift versus calculated molecular dipole moment for a smaller subset of these same alkanethiol modifiers on silver are also shown in Figure 3 (triangle symbols). The vacuum level shifts are offset from the series on gold, however, the shifts in local vacuum vs change in $D_{\perp,SAM}$ are nearly the same (-0.55 eV/D on silver vs -0.65 eV/D on gold). These differences in slope might be within expected experimental uncertainties, or may be a reflection of differences in the areal density of alkanethiol modifiers (N) in eq 1.[24,32−34] For adsorption of a modifier with zero molecular dipole moment ($D_{\perp,SAM,Ag} = 0$), $\Delta\Phi_{vac} = +0.49$ eV. The vacuum level shift for adsorption of xenon on silver is -0.44 to -0.47 eV,[55,81] similar to the shifts seen for xenon adsorption on gold. Simple physisorption of a nonpolar modifier on Ag is therefore not the likely originator of the difference in vacuum level shifts at $D_{\perp,SAM} = 0$ for these two metals.[24,32−34]

From these data for $D_{\perp,SAM,Au} = 0$, where there is no contribution from the molecular dipole we infer, as in previous studies, that the vacuum level shift from the thiol bond is comparable to that seen for a noninteracting adsorbate (e.g., xenon) and[6,77]

$$\Delta\Phi_{vac} = eD_{total} = -N[D_{Au-S}/\varepsilon_0 \cdot \varepsilon_{Au-S}] = 0 \text{ eV} \quad (2)$$

which suggests a BD shift for the Au−S bond $e\mu_{Au-S} \approx 0$ eV, consistent with a nearly covalent bond for gold thiolates.

The larger vacuum level shift from the Ag−S bond:

$$\Delta\Phi_{vac} = eD_{total} = -N[D_{Ag-S}/\varepsilon_0 \cdot \varepsilon_{Ag-S}] = +0.49 \text{ eV} \quad (3)$$

In this case the measured vacuum level shift (+0.49 eV), minus the expected vacuum level shift for a noninteracting adsorbate on Ag ($\Delta\Phi_{vac}$ for xenon $= -0.46$ eV) provides an estimate of a total BD shift of 0.9 eV, consistent with the more ionic character for silver thiolate bond.[22,82−85]

Thiolates tend to bond to gold with sp^3 hybridization, resulting in a Au−S−C bond angle closer to 104°, with energetically favorable bonding at on-top sites. Thiolates on silver typically bond in a mixture of sp^3 and sp bonding geometries, resulting in Ag−S−C bond angles of 104° and 180°, respectively.[22,82−85] Alkanethiolates exhibit bonding to both on-top and 3-fold hollow sites, allowing for a more effective packing structure with the molecular axis much closer to the surface normal.

One of the observables from our studies of the normal alkanethiol modifiers was the shift in effective work function with increasing alkanethiol chain length. Previous Kelvin probe studies have produced slopes of 9.3, 14.1, and 20 mV/CH_2 unit for alkanethiol monolayers on gold.[78,86−88] Using UPS studies on gold we observed the slope was 19 mV/CH_2,[6] but on silver we observed the slope to be 39 mV/CH_2 unit. Since the tilt angle on silver is lower, the actual SAM thickness increases slightly more for each additional methylene unit but not to the extent that completely explains this difference (ca. 15% vs 100%).

As expected, odd−even effects seen for these modifiers on gold surfaces are reproduced for silver surfaces, with nearly the same magnitude and direction as seen for odd−even chains on gold. The low KE UPS cutoff, and therefore the effective work function, are higher for the odd chain length $-CF_3$ terminated alkanethiols on gold.[6] The difference in effective work function, proceeding from odd chain length to even chain length modifiers on silver is ca. 0.2 eV, similar to the differences previously seen on gold surfaces. It was hypothesized that this family of alkanethiols on silver would reverse the odd−even order of these surface dipole effects, since chain tilt angles on silver are different from those on gold resulting in different terminal methylene orientations (Figure 4).[22] Instead the odd $-CF_3$-terminated alkanethiol SAM has the larger negative dipole moment on both silver and gold.

We also note the similarity in these data with recent studies of the modification of indium−tin oxide (ITO) thin films with a series of normal and fluorinated phenyl-phosphonic acids (PAs).[7−9] These studies have shown that the effective work function of ITO can be tuned in a fashion similar to the Au and Ag surfaces discussed here. The slope, $\Delta\Phi_{vac}/\Delta\mu$ for these PA-modified ITO surfaces is nearly identical to the slope seen for Ag surfaces, and the effective work function can be tuned over a range of ca. 1.2 eV. The origin of these similarities appears to arise in part from the small bond dipoles in the thiolates or phosphonate bonds, which add predictably and linearly to the molecular dipole moment of the alkyl or aryl surface modifiers.[7−9]

UPS Studies of Mixed Monolayers of C16F2/C16. In this section we show that the effective work function of gold surfaces can be precisely tuned by simple mixing of **C16F2** and **C16** (Figure 5). Monolayers of varying concentrations of **C16F2** in **C16** on clean Au surfaces were characterized using UV and X-ray photoelectron spectroscopy. Film compositions were created from 0% to 100% **C16F2** in 10% increments with additional concentrations of 5% and 95% **C16F2**. The relative **C16F2** composition in each monolayer was verified using the peak areas of F(1s) X-ray photoelectron spectra. Surface compositions tracked solution composition reasonably well, however, a slight enhancement of the normal alkane was observed when the solution concentrations were between 40:60 and 60:40 (see Supporting Information). We used the measured mole percentage of **C16F2** as the x-axis in Figure 5b. A linear relationship is observed between the increase in mol % **C16F2** and the vacuum level shift, and the linearity of these shifts with concentration suggest that the vacuum level, and therefore the Schottky barrier height for charge injection, can be tuned to ±0.1 eV.

Several investigators have discussed how the dipole fields within a self-assembled monolayer can be dissipated via charge redistribution, so that the effective work function shift is not as great as might be expected from close-packed layers of aligned dipoles.[70−72] Other investigators have discussed the possible role of polarization effects to dissipate the dipole field, especially for aromatic surface modifiers.[1,2,89] While these effects may indeed be present for highly polarizable modifiers or modifiers with highly electron donating or accepting termini, it is interesting that our effective work function data changes linearly even at very low or very high concentrations of the **C16F2** modifier, suggesting that the tunability in effective work function remains entirely predictable even when the semifluorinated modifier is completely isolated from comparable modifiers.

We also modeled the change in surface potential experienced by an escaping photoelectron from a self-assembled monolayer with a low mole percentage of the **C16F2** alkanethiol (Supporting Information, Figure S1). In this simple simulation we estimated the dipolar field experienced by a photoelectron escaping from the middle of a monolayer with ca. 400

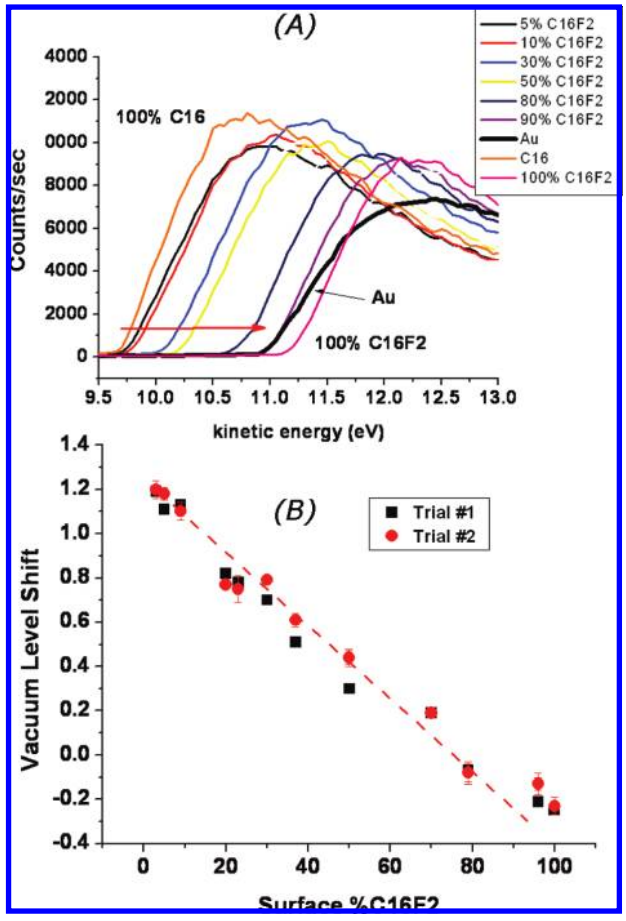

Figure 5. (a) Expanded view of the low KE region for UPS of clean Au and Au surfaces modified with mixtures of **C16** and **C16F2** alkanethiols. The effective work function for the Au surface modified with 100% **C16F2** is higher than for clean Au. (b) Vacuum level shift (shift in the low KE edge from (a)) as a function of mol % **C16F2** in the mixed thiol films (two trials are shown to indicate the precision in these measurements). Composition of the thin films as a function of solution composition is shown in Supporting Information.

molecules, with variable fraction of **C16F2** vs **C16** chains, all isolated from each other. Each alkanethiol was treated as a point dipole. The center-to-center distance between each chain was estimated to be 5 Å and the calculation was summed over an ensemble of molecules roughly 11 chains to each side of a molecule in the center of the thin film array. The potential was calculated for an electron leaving the surface at a range of distances from the terminus of the alkanethiol chains, specifically 0.5, 1, 2, 5, and 10 nm. The estimated potential experienced at a distance of 1 nm from the surface (Figure S2), as a function of mole percentage **C16F2** showed the same linear correlation between composition, surface potential, and shift in effective vacuum level as seen in Figure 5, suggesting that a point dipole model provides a reasonable description to the local vacuum level shifts seen in the photoemission experiments.

Conclusion

SAMs derived from ω-functionalized alkanethiols were used to tune the effective work function of gold over a range of ca. 1.8 eV using mixtures of methyl-terminated alkanethiols (**C16**) and alkanethiols fluorinated at the two terminal carbon atoms (**C16F2**). UPS was used to monitor changes in effective work function, using shifts in the low KE edge of these photoemission spectra to give an indication of the shift in local vacuum level due to the interface dipole effect created by the surface modifier. A simple point dipole model was applied to rationalize these apparent shifts in vacuum level with mixed monolayers of **C16F2** and **C16** alkanethiols. Terminally functionalized alkanethiols, where the terminal group varies from $-CH_3$, to $-$phenyl, $-Cl$, $-Br$, and $-CF_3$ or $-CF_2CF_3$, caused a shift in local vacuum level that varied linearly with the molecular dipole of the individual modifiers both on gold and silver surfaces. The studies presented here suggest that the intrinsic dipole in the gold$-$thiolate bond is quite small (less than 50 meV), whereas the silver$-$thiolate bond has a strong polar character in the direction Ag^+-S^- with a magnitude of ca. 900 meV.

Acknowledgements. .

This work was supported in part by (N.R.A.) the National Science Foundation CHE-0517963, the NSF Science and Technology Center-Materials and Devices for Information Technology$-$DMR-0120967, and the Office of Naval Research; and (J.E.P.) the National Science Foundation CHE-0848624. The work performed at the University of Houston was generously supported by the Robert A. Welch Foundation (E-1320) and the National Science Foundation (DMR-0906727).

Supporting Information Available: Schematics showing the potential felt by a photoelectron leaving a mixed alkanethiol monolayer (Figure S1), the estimated potential felt by this photoelectron as a function of composition of the thiol monolayer(s) (Figure S2), the mole percent of **C16F2** found in each film (determined from XPS) as a function of solution composition (Figure S3), and RAIRS spectra of these alkanethiols on Ag (Figures S4 and S5 and Table S1). This material is available free of charge via the Internet at http://pubs.acs.org.

References and Notes

(1) Heimel, G.; Romaner, L.; Zojer, E.; Bredas, J. -L. *Acc. Chem. Res.* **2008**, *41*, 721–729.
(2) Heimel, G.; Romaner, L.; Bredas, J. L.; Zojer, E. *Langmuir* **2008**, *24*, 474–482.
(3) Heimel, G.; Romaner, L.; Bredas, J. L.; Zojer, E. *Surf. Sci.* **2006**, *600*, 4548–4562.
(4) de Boer, B.; Hadipour, A.; Mandoc, M. M.; van Woudenbergh, T.; Blom, P. W. M. *Adv. Mater.* **2005**, *17*, 621–625.
(5) De Renzi, V.; Rousseau, R.; Marchetto, D.; Biagi, R.; Scandolo, S.; del Pennino, U. *Phys. Rev. Lett.* **2005**, *95*.
(6) Alloway, D. M.; Hofmann, M.; Smith, D. L.; Gruhn, N. E.; Graham, A. L.; Colorado, R.; Wysocki, V. H.; Lee, T. R.; Lee, P. A.; Armstrong, N. R. *J. Phys. Chem. B* **2003**, *107*, 11690–11699.
(7) Paniagua, S. A.; Hotchkiss, P. J.; Jones, S. C.; Marder, S. R.; Mudalige, A.; Marrikar, F. S.; Pemberton, J. E.; Armstrong, N. R. *J. Phys. Chem. C* **2008**, *112*, 7809–7817.
(8) Paramonov, P. B.; Paniagua, S. A.; Hotchkiss, P. J.; Jones, S. C.; Armstrong, N. R.; Marder, S. R.; Bredas, J. L. *Chem. Mater.* **2008**, *20*, 5131–5133.
(9) Hotchkiss, P. J.; Hong, L.; Pavel, B. P.; Sergio, A. P.; Simon, C. J.; Neal, R. A.; Jean-Luc, B.; Seth, R. M. *Adv. Mater.* 2009, in press.
(10) Salomon, A.; Boecking, T.; Seitz, O.; Markus, T.; Amy, F.; Chan, C.; Zhao, W.; Cahen, D.; Kahn, A. *Adv. Mater.* **2007**, *19*, 445–450.
(11) Salomon, A.; Bocking, T.; Gooding, J.; Cahen, D. *Nano Lett.* **2006**, *6*, 2873–2876.
(12) Gershewitz, O.; Grinstein, M.; Sukenik, C. N.; Regev, K.; Ghabboun, J.; Cahen, D. *J. Phys. Chem. B* **2004**, *108*, 664–672.
(13) Vilan, A.; Ghabboun, J.; Cahen, D. *J. Phys. Chem. B* **2003**, *107*, 6360–6376.
(14) Salomon, A.; Cahen, D.; Lindsay, S.; Tomfohr, J.; Engelkes, V. B.; Frisbie, C. D. *Adv. Mater.* **2003**, *15*, 1881–1890.
(15) Cahen, D.; Kahn, A. *Adv. Mater.* **2003**, *15*, 271–277.
(16) Vilan, A.; Cahen, D. *Trends Biotechnol.* **2002**, *20*, 22–29.
(17) Ishii, H.; Sugiyama, K.; Ito, E.; Seki, K. *Adv. Mater.* **1999**, *11*, 605–625.
(18) Duhm, S.; Heimel, G.; Salzmann, I.; Glowatzkl, H.; Johnson, R. L.; Vollmer, A.; Rabe, J. P.; Koch, N. *Nat. Mater.* **2008**, *7*, 326–332.
(19) Romaner, L.; Heimel, G.; Zojer, E. *Phys. Rev. B* **2008**, *77*, 045113.

(20) Rangger, G. M.; Romaner, L.; Heimel, G.; Zojer, E. *Surf. Interface Anal.* **2008**, *40*, 371–378.
(21) Koch, N.; Gerlach, A.; Duhm, S.; Glowatzki, H.; Heimel, G.; Vollmer, A.; Sakamoto, Y.; Suzuki, T.; Zegenhagen, J.; Rabe, J. P.; Schreiber, F. *J. Am. Chem. Soc.* **2008**, *130*, 7300–7304.
(22) Tao, F.; Bernasek, S. L. *Chem. Rev.* **2007**, *107*, 1408–1453.
(23) Cornil, D.; Olivier, Y.; Geskin, V.; Cornil, J. *Adv. Funct. Mater.* **2007**, *17*, 1143–1148.
(24) Rusu, P. C.; Brocks, G. *Phys. Rev. B* **2006**, *74*, 073414.
(25) Wold, D. J.; Haag, R.; Rampi, M. A.; Frisbie, C. D. *J. Phys. Chem. B* **2002**, *106*, 2813–2816.
(26) Chabinyc, M. L.; Chen, X. X.; Holmlin, R. E.; Jacobs, H.; Skulason, H.; Frisbie, C. D.; Mujica, V.; Ratner, M. A.; Rampi, M. A.; Whitesides, G. M. *J. Am. Chem. Soc.* **2002**, *124*, 11730–11736.
(27) Hanson, E. L.; Guo, J.; Koch, N.; Schwartz, J.; Bernasek, S. L. *J. Am. Chem. Soc.* **2005**, *127*, 10058–10062.
(28) Bruner, E. L.; Koch, N.; Span, A. R.; Bernasek, S. L.; Kahn, A.; Schwartz, J. *J. Am. Chem. Soc.* **2002**, *124*, 3192–3193.
(29) Heimel, G.; Romaner, L.; Zojer, E.; Bredas, J. L. *Nano Lett.* **2007**, *7*, 932–940.
(30) Natan, A.; Kronik, L.; Haick, H.; Tung, R. T. *Adv. Mater.* **2007**, *19*, 4103–4117.
(31) Risko, C.; Zangmeister, C. D.; Yao, Y.; Marks, T. J.; Tour, J. M.; Ratner, M. A.; van Zee, R. D. *J. Phys. Chem. C* **2008**, *112*, 13215–13225.
(32) Rusu, P. C.; Brocks, G. *J. Phys. Chem. B* **2006**, *110*, 22628–22634.
(33) Rusu, P. C.; Giovannetti, G.; Brocks, G. *J. Phys. Chem. C* **2007**, *111*, 14448–14456.
(34) Rusu, M.; Gasiorowski, J.; Wiesner, S.; Meyer, N.; Heuken, M.; Fostiropoulos, K.; Lux-Steiner, M. C. *Thin Solid Films* **2008**, *516*, 7160–7166.
(35) Venkataraman, N. V.; Zurcher, S.; Rossi, A.; Lee, S.; Naujoks, N.; Spencer, N. D. *J. Phys. Chem. C* **2009**, *113*, 5620–5628.
(36) DiBenedetto, S. A.; Facchetti, A.; Ratner, M. A.; Marks, T. J. *Adv. Mater.* **2009**, *21*, 1407–1433.
(37) Ballav, N.; Terfort, A.; Zharnikov, M. *J. Phys. Chem. C* **2009**, *113*, 3697–3706.
(38) Romaner, L.; Heimel, G.; Ambrosch-Draxl, C.; Zojer, E. *Adv. Funct. Mater.* **2008**, *18*, 3999–4006.
(39) Beebe, J. M.; Kim, B.; Frisbie, C. D.; Kushmerick, J. G. *Acs Nano* **2008**, *2*, 827–832.
(40) Wang, J. G.; Prodan, E.; Car, R.; Selloni, A. *Phys. Rev. B* **2008**, *77*.
(41) Ivanco, J.; Zahn, D. R. T. *J. Vac. Sci. Technol., A* **2009**, *27*, 1178–1182.
(42) Hwang, J.; Wan, A.; Kahn, A. *Mat. Sci. Eng., R: Reports* **2009**, *64*, 1–31.
(43) Thieblemont, F.; Seitz, O.; Vilan, A.; Cohen, H.; Salomon, E.; Kahn, A.; Cahen, D. *Adv. Mater.* **2008**, *20*, 3931+.
(44) Ulman, A. *Chem. Rev.* **1996**, *96*, 1533–1554.
(45) Campbell, I. H.; Kress, J. D.; Martin, R. L.; Smith, D. L.; Barashkov, N. N.; Ferraris, J. P. *Appl. Phys. Lett.* **1997**, *71*, 3528–3530.
(46) Campbell, I. H.; Rubin, S.; Zawodzinski, T. A.; Kress, J. D.; Martin, R. L.; Smith, D. L.; Barashkov, N. N.; Ferraris, J. P. *Phys. Rev. B* **1996**, *54*, 14321–14324.
(47) Stoliar, P.; Kshirsagar, R.; Massi, M.; Annibale, P.; Albonetti, C.; de Leeuw, D. M.; Biscarini, F. *J. Am. Chem. Soc.* **2007**, *129*, 6477–6484.
(48) Kline, R. J.; Mcgehee, M. D.; Toney, M. F. *Nat. Mater.* **2006**, *5*, 222–228.
(49) Chen, W.; Huang, C.; Gao, X. Y.; Wang, L.; Zhen, C. G.; Qi, D. C.; Chen, S.; Zhang, H. L.; Loh, K. P.; Chen, Z. K.; Wee, A. T. S. *J. Phys. Chem. B* **2006**, *110*, 26075–26080.
(50) Akkerman, H. B.; Naber, R. C. G.; Jongbloed, B.; van Hal, P. A.; Blom, P. W. M.; de Leeuw, D. M.; de Boer, B. *Proc. Natl. Acad. Sci. U.S.A.* **2007**, *104*, 11161–11166.
(51) de Boer, B.; Frank, M. M.; Chabal, Y. J.; Jiang, W. R.; Garfunkel, E.; Bao, Z. *Langmuir* **2004**, *20*, 1539–1542.
(52) Sharma, A.; Kippelen, B.; Hotchkiss, P. J.; Marder, S. R. *Appl. Phys. Lett.* **2008**, *93*, 163308.
(53) Smith, D. L.; Wysocki, V. H.; Colorado, R.; Shmakova, O. E.; Graupe, M.; Lee, T. R. *Langmuir* **2002**, *18*, 3895–3902.
(54) Wandelt, K. *Appl. Surf. Sci.* **1997**, *111*, 1–10.
(55) Ishi, S.; Viswanathan, B. *Thin Solid Films* **1991**, *201*, 373–402.
(56) Porter, M. D.; Bright, T. B.; Allara, D. L.; Chidsey, C. E. D. *J. Am. Chem. Soc.* **1987**, *109*, 3559–3568.
(57) Lee, S.; Puck, A.; Graupe, M.; Colorado, R.; Shon, Y. S.; Lee, T. R.; Perry, S. S. *Langmuir* **2001**, *17*, 7364–7370.
(58) Tamada, K.; Ishida, T.; Knoll, W.; Fukushima, H.; Colorado, R.; Graupe, M.; Shmakova, O. E.; Lee, T. R. *Langmuir* **2001**, *17*, 1913–1921.
(59) Houssiau, L.; Graupe, M.; Colorado, R.; Kim, H. I.; Lee, T. R.; Perry, S. S.; Rabalais, J. W. *J. Chem. Phys.* **1998**, *109*, 9134–9147.
(60) Sobkowski, J.; Smolinski, S.; Zelenay, P. *Colloids Surf., A* **1998**, *134*, 39–45.
(61) Smolinski, S.; Zelenay, P.; Sobkowski, J. *J. Electroanal. Chem.* **1998**, *442*, 41–47.
(62) Tiani, D. J.; Pemberton, J. E. *Langmuir* **2003**, *19*, 6422–6429.
(63) Lyon, J. E.; Cascio, A. J.; Beerbom, M. M.; Schlaf, R.; Zhu, Y.; Jenekhe, S. A. *Appl. Phys. Lett.* **2006**, *88*.
(64) Schlaf, R.; Murata, H.; Kafafi, Z. H. *J. Electron Spectrosc. Relat. Phenom.* **2001**, *120*, 149–154.
(65) Schlaf, R.; Parkinson, B. A.; Lee, P. A.; Nebesny, K. W.; Armstrong, N. R. *J. Phys. Chem. B* **1999**, *103*, 2984–2992.
(66) Alloway, D. M. Ph.D. Dissertation, University of Arizona 2008.
(67) Schmidt, M. W.; Baldridge, K. K.; Boatz, J. A.; Elbert, S. T.; Gordon, M. S.; Jensen, J. H.; Koseki, S.; Matsunaga, N.; Nguyen, K. A.; Su, S. J.; Windus, T. L.; Dupuis, M.; Montgomery, J. A. *J. Comput. Chem.* **1993**, *14*, 1347–1363.
(68) Heinz, R.; Rabe, J. P. *Langmuir* **1995**, *11*, 506–511.
(69) Laibinis, P. E.; Whitesides, G. M.; Allara, D. L.; Tao, Y. T.; Parikh, A. N.; Nuzzo, R. G. *J. Am. Chem. Soc.* **1991**, *113*, 7152–7167.
(70) Fragouli, D.; Kitsopoulos, T. N.; Chiodo, L.; Della Sala, F.; Cingolani, R.; Ray, S. G.; Naaman, R. *Langmuir* **2007**, *23*, 6156–6162.
(71) Neuman, O.; Naaman, R. *J. Phys. Chem. B* **2006**, *110*, 5163–5165.
(72) Ray, S. G.; Cohen, H.; Naaman, R.; Liu, H. Y.; Waldeck, D. H. *J. Phys. Chem. B* **2005**, *109*, 14064–14073.
(73) Guo, J.; Koch, N.; Schwartz, J.; Bernasek, S. L. *J. Phys. Chem. B* **2005**, *109*, 3966–3970.
(74) Span, A. R.; Bruner, E. L.; Bernasek, S. L.; Schwartz, J. *Langmuir* **2001**, *17*, 948–952.
(75) Li, J. F.; Wang, L.; Liu, J.; Evmenenko, G.; Dutta, P.; Marks, T. J. *Langmuir* **2008**, *24*, 5755–5765.
(76) Marrikar, F. S.; Brumbach, M.; Evans, D. H.; Lebron-Paler, A.; Pemberton, J. E.; Wysocki, R. J.; Armstrong, N. R. *Langmuir* **2007**, *23*, 1530–1542.
(77) Crispin, X.; Geskin, V.; Crispin, A.; Cornil, J.; Lazzaroni, R.; Salaneck, W. R.; Bredas, J. L. *J. Am. Chem. Soc.* **2002**, *124*, 8131–8141.
(78) Evans, S. D.; Ulman, A. *Chem. Phys. Lett.* **1990**, *170*, 462–466.
(79) Linder, B.; Kromhout, R. A. *J. Phys. Chem. A* **2003**, *107*, 3270–3276.
(80) McElhiney, G.; Pritchard, J. *Surf. Sci.* **1976**, *60*, 397–410.
(81) McElhiney, G.; Papp, H.; Pritchard, J. *Surf. Sci.* **1976**, *54*, 617–634.
(82) Kruger, D.; Fuchs, H.; Rousseau, R.; Marx, D.; Parrinello, M. *J. Chem. Phys.* **2001**, *115*, 4776–4786.
(83) Li, T. W.; Chao, I.; Tao, Y. T. *J. Phys. Chem. B* **1998**, *102*, 2935–2946.
(84) Sellers, H.; Ulman, A.; Shnidman, Y.; Eilers, J. E. *J. Am. Chem. Soc.* **1993**, *115*, 9389–9401.
(85) Zhang, L. Z.; Goddard, W. A.; Jiang, S. Y. *J. Chem. Phys.* **2002**, *117*, 7342–7349.
(86) Lu, J.; Delamarche, E.; Eng, L.; Bennewitz, R.; Meyer, E.; Guntherodt, H. J. *Langmuir* **1999**, *15*, 8184–8188.
(87) Ratner, M. *Nature* **2000**, *404*, 137–138.
(88) Ratner, M. *Nature* **2005**, *435*, 575–577.
(89) Romaner, L.; Heimel, G.; Bredas, J. L.; Gerlach, A.; Schreiber, F.; Johnson, R. L.; Zegenhagen, J.; Duhm, S.; Koch, N.; Zojer, E. *Phys. Rev. Lett.* **2007**, *99*, 256801.

JP909494R